



A Multi-objective Design Optimization Approach to PV and Battery Storage for Sector-Integrated Energy Systems at Logistics Facilities - Under Consideration for the Integration of Temperature-controlled Transport

Jan-Simon Telle^(✉), Sunke Schlüters, Thomas Poppinga, Benedikt Hanke, Karsten von Maydell, and Carsten Agert

German Aerospace Center (DLR), Institute for Networked Energy Systems, Stuttgart, Germany
jan-simon.telle@dlr.de

Abstract. This work outlines an approach to the optimal design optimization of a photovoltaic (PV) and battery storage system and its integration into the sector-integrated energy system of a logistics company's facilities. Another major objective is the optimized integration of refrigerated trailers (reefers) into the energy system with the goal of minimizing both costs and CO₂ emissions, as demonstrated in a case study. For this purpose, an existing energy system model utilizing reefers was optimized for computing time and the energy system was extended through the use of a facility's cooling utility. Multi-criteria design optimization was performed using a multi-objective evolutionary algorithm based on decomposition (MOEDA/D) approach. For this, three key performance indicators (KPIs) were used: the annuity, CO₂ emissions, and own-consumption rate. The results of the multi-criteria design optimization were then analyzed using Pareto fronts. Stakeholders are thus able to find their individual techno-economic/ecological optimum and so plan the transformation to an decentralized, renewable, distributed energy supply accordingly. Three selected Pareto optimal results were selected to evaluate the effect of PV and battery storage on the optimal operation of the sector-integrated energy system and reefer integration.

Keywords: Multi-objective design optimization · sector-integrated energy system · PV and battery storage · temperature-controlled transportation · Pareto fronts

1 Introduction

1.1 Background

The electrification of an increasing number of sectors leads to corresponding challenges for electrical grids due to an overall increasing energy demand, missing simultaneity between generation and consumption, and load peaks that result. Decentralized, sector-integrated systems can be a solution in many areas to reduce grid expansion and advance

© The Author(s) 2023

P. Schossig et al. (Eds.): IRES 2022, AHE 16, pp. 451–469, 2023.

https://doi.org/10.2991/978-94-6463-156-2_29

the energy transition [1]. This also affects logistics companies, which must integrate renewable energies solutions into both their vehicle fleets and facilities. Distributed generation and storage systems will play a key role in this transformation.

Sector-coupling or the sector-integrated decentralized energy systems offers a solution path to mastering the challenges of the energy transition. The coupling of the electricity, heating, cooling, and transportation sectors offers the possibility of substituting fossil energy sources with renewable ones. The integration of renewable energy sources requires a high degree of flexibility and load management solutions. Solutions must also be found for the transportation sector in particular, so that it can also be integrated into decentralized, sector-integrated energy systems [2, 3], and [4].

An increasingly important driver of decentralized solutions is the cost of fossil fuels which, on the one hand, has seen a sharp increase in recent months and, on the other, is expected to rise in the near future due to the national CO₂ pricing of Germany [5] and the EU's CO₂ certificate trading system [6]. Due to the uncertainty of prices in energy procurement, energy self-sufficiency is also becoming increasingly appealing to small- and medium-sized enterprises (SME), as well as industrial companies, increasing the demand for solutions for decentralized generation and storage at company sites. It is therefore becoming increasingly important for logistics and other companies to substitute as many fossil energy sources as possible, such as fuels for transport, in a decentralized manner, e.g., by carrying out pre-conditioning processes for temperature-controlled vehicles. For this, the present study offers a modeling approach for achieving the transformation of an existing, conventional energy system into an optimized, distributed and integrated one.

1.2 Related Work

The demand for temperature-controlled transportation has been increasing in recent years, as shown by the number of registered refrigerated trailers (reefers) identified in market analyses [7, 8].

With rising fossil fuel prices [9] and increasing pressure to reduce greenhouse gas emissions through the shortage of certificates [6], fossil energy sources must be substituted where possible.

In 2015, CE Delft presented a study which showed that the electric cooling of refrigerated transport vehicles can save 290–580 kt/CO₂ during their idling time [10]. However, the technical prerequisites for the electric conditioning of reefers mean that they are often still operated by diesel and thus produce more emissions, are less energy-efficient, and are significantly noisier [11, 12].

In research, the integration of all sectors and concepts for green logistics to reduce emissions, e.g., in temperature-controlled transport, is currently attracting widespread interest [13].

Rai et al. evaluated the environmental impact and energy demand of diesel-fueled, temperature-controlled, over-the-road transportation and compared it to alternative refrigeration technologies in the food distribution sector [11, 14], and [15]. In [11], a method is also presented for modeling a reefer and calculating its energy demand.

Schmeling et al. present a generalized methodology for optimizing the design of distributed energy systems [16]. In their exhaustive literature review, they outline the main approaches to design optimization that have been used thus far. They found that a

multi-objective evolutionary algorithm based on decomposition (MOEDA/D) approach has not yet been employed. The Python library *PyGMO* [17] was used for design optimization of different technologies for a distributed energy system. The energy system was modeled in *oemof.solph* [18] and a linear optimizer is used to optimize the operating strategies of the system [16]. Meanwhile, Schönfeldt presents a techno-socio-economic Pareto approach to energy system optimization [17]. Both studies present how results can be analyzed with several key performance indicators (KPIs) using Pareto fronts.

This study also draws on the method presented in [16] and [17].

1.3 Contribution

In this paper, we present a refined model of the sector-integrated energy system of a logistics property from [18] based on the open energy modeling framework (*oemof*). The focus of the modeling aspect is the computing time-optimized model of the preconditioning process of reefers and the integration of cooling demand and supply into a sector-integrated energy system.

For the optimized integration of reefers into a local energy system, we present an approach to the multi-criteria design optimization of a PV and battery storage system. For this, we employ the KPIs of annuity, CO₂ emissions, and degree of PV own-consumption rate and evaluate the Pareto-optimal results.

Using the example of a case study of the distributed energy system of a logistics facility, we highlight the developments resulting from the transformation of a conventional energy supply towards a sector-integrated one.

In a previous work by the authors, a method was presented for estimating the energy demand of refrigerated trailers based on telematics data [18]. Furthermore, the modeling of a sector-integrated energy system, with a focus on the reefer component, was presented. With the help of a linear optimizer, the overall energy system was then optimized for its costs. In contrast, the focus of this work is on the *design optimization* of a PV and battery storage system within a sector-integrated energy system that takes into account the integration of the reefer preconditioning processes.

2 Methodology

2.1 Case Study

For this study, a logistics facility in Lower Saxony was considered that is in the process of changing its energy supply from a conventional fuel-based one to a sector-integrated, mostly electric supply. In particular, the integration of temperature-controlled transports is considered (Fig. 1).

This means that in addition to the electricity, heating, cooling, and passenger transport sectors, the logistics sector is also considered in the analysis of the local energy system. Here, the preconditioning processes of reefers, which were previously supplied by diesel, are powered by the local electrical grid. Tractors are not taken into account, as they are not refueled on-site. The electricity supply currently consists of an electrical load at the logistics facility buildings and a connection point to the public grid. In future, it should be complemented by a PV and battery storage system.

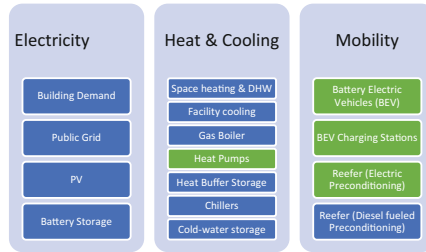


Fig. 1. Overview of the components of the observed energy system (blue: conventional; green: additional to the sector-integrated energy system).

The heat demand (space heating, domestic hot water and air conditioning) is initially met by gas boilers and a connection to the public natural gas network. In the second step, heat pumps and hot water buffer storage are integrated into the system, with the gas boilers reserved for peak load coverage alone. The cooling demand is met by heat pumps (chillers) combined with a cold water storage capacity.

In terms of the personal transportation of the logistics company, the fleet will be converted from fuel-driven to battery–electric vehicles (BEVs) and a charging infrastructure will be integrated into the local energy system.

As an additional electrical consumer, reefers that must be preconditioned to a specific target temperature (set-point) will be connected to the electrical system on-site. Once the set-point is reached, the reefers will be disconnected and no longer considered part of the energy system.

For the energy system described, the optimal size of distributed PV generation and storage is evaluated. Two different scenarios are considered (Table 1): a conventional case in which the preconditioning processes of the reefers are conducted using diesel and one in which the reefers are electrically-connected to a decentralized grid. In addition to the goal of the optimized integration of the reefer, the question of the influence of parallel developments in other areas of the energy system on the design optimization of PV and battery storage configurations will be investigated, i.e., what influence does the conversion of personal transport in favor of BEVs or the heat supply to heat pumps have on the results of the design optimization? The analysis of the design optimization is based on three KPIs, namely: annuity, CO₂ emissions, and own-consumption rate.

Table 1. Scenario definition.

Scenario	Description
Conventional energy system (CES)	Gas-covered heat demand, no BEVs, no heat pumps, diesel-fueled reefer pre-conditioning processes
Sector-integrated energy system (SIES)	Sector-integration, electric reefer pre-conditioning

Table 2. Energy demand per sector during the observation period (01/07/2021 to 30/06/2022).

Sector	In MWh
Electricity	178.62
Heat	281.13
Cooling	12.74
Mobility (BEV)	58.58

In the case study, fixed time series of electricity, heating and cooling demand for a period of one year (01/07/2021 to 30/06/2022) were used. Table 2 shows the annual energy demand of the different sectors. Data from the ELogZ research project was used as the basis for the electricity, heat and cooling load profiles [19].

For the modeling of the PV system, the Python library `pv_lib` was used [20], with weather reports for irradiance (GHI, DNI, DHI), wind speed, and ambient temperature time series from Open DWD employed [21].

The calculation of the coefficient of performance (COP) of the heat pumps and energy efficiency ratio (EER) of the chillers was performed in accordance with [22].

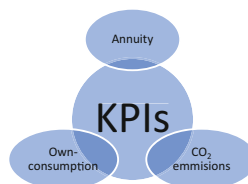
Variable consumers such as BEVs and reefers that are only temporarily on-site do not have a fixed consumption time series. When a reefer is preconditioned or a BEV loaded is determined by the optimizer. The calculations of the energy demand of the BEV and reefer charging or preconditioning processes were performed on the basis of project results [19] and own calculations and can be traced in [18].

2.2 Key Performance Indicators

Three KPIs were used for the multi-criteria design optimization (Fig. 2): The annuity, CO₂ emissions, and PV own-consumption rate (OCR) of the energy system. The goal of optimization is to minimize costs and emissions and maximize the OCR.

2.2.1 Annuity

The annuity A_N is calculated according to part 1 of guideline VDI 2067 [23] and [16], which describes the basics of the economic efficiency of building installations and is used in this study to calculate the annuity of PV and battery storage systems.

**Fig. 2.** Overview of the KPIs.

The design of a PV and battery storage system includes the annuity of capital-related and operation-related costs (A_C and A_{OP}), as well as proceeds A_P (Eq. 1):

$$A_N = A_C + A_{OP} - A_P \tag{1}$$

The capital-related costs were calculated as follows:

$$A_C = (A_0 + A_1 + \dots + A_n - RV) \cdot a \tag{2}$$

where A_0 is the cash value of the initial investment, A_1 to A_n are the cash values of replacements within the observation period, and RV is the residual value of the investment.

The annuity factor is obtained from Eq. 3:

$$a = \frac{(q - 1)}{(1 - q^{-T})} \tag{3}$$

The interest rates, price change factor and observation period used herein are listed in Table 3.

The residual value RV can be calculated as shown in Eq. 4:

$$RV = A_0 \cdot r^{n \cdot T_{SL}} \cdot \frac{(n + 1) \cdot T_{SL} - T}{T_{SL}} \tag{4}$$

Table 3. General parameters for calculating the annuity.

General Parameters	Values
Observation period T	10 years
Interest factor q	1.060
Price change factor r	1.027

Table 4. Calculation parameters for determining the operation-related costs.

	PV	Battery
T_{SL}	20	10
f_M	0.005	0.01
$f_{S,In}$	0.005	0.01

Table 5. Assumptions of the EEG remuneration according to plant size [24].

PV Size	EEG remuneration
Up to 10 kW	0.0624
Up to 40 kW	0.0606
Up to 750 kW	0.0514

Table 6. CO₂ emission factors for the German electricity mix, natural gas and diesel.

<i>Energy source</i>	<i>CO₂ emissions factor [g/kWh]</i>
Electricity mix [28]	420
Natural Gas [29]	182
Diesel [29]	266

where a is the annuity factor, T_{SL} the service life of the energy system in years, T the period under consideration in years, interest factor, price change factor, and number of replacements n , whereby the number of replacements n is calculated from the ratio of T to T_{SL} . For the initial investment costs A_0 , internal project calculations were used [19].

The calculation of the operating costs was carried out according to Eq. 5:

$$A_{OP} = A_0 \cdot (f_M + f_S) \quad (5)$$

where f_R is the factor for the repair effort and f_{S+Insp} the factor for service and inspection.

The proceeding A_P that can be generated by the EEG funding or day-ahead prices for PV systems when it is fed into the grid is calculated as shown in Eq. 6:

$$A_P = E_1 \cdot a \cdot b_E \quad (6)$$

where E_1 is the proceedings of the first year and b_E the price dynamic cash value factor for proceeds (Eq. 7).

$$b_E = \frac{1 - \left(\frac{r}{q}\right)^T}{q - r} \quad (7)$$

As the installed power of the PV plant exceeds 100 kW, according to EEG § 10b, this must be accounted for in direct marketing efforts [25]. A revenue of € 0.0601/kWh is assumed from direct marketing, corresponding to the EEG reference values for payments for PV [26], minus a direct marketing service charge of € 0.004/kWh, according to [27], for PV electricity fed into the grid.

2.2.2 CO₂ Emissions

CO₂ emissions within the period under consideration are calculated using the CO₂ emission factors for the German electricity mix, natural gas, and diesel, as shown in Table 6.

The calculation is performed by multiplying the required energy quantities of grid electricity, natural gas and diesel by the respective emission factors (Table 6) and a subsequent summation.

2.2.3 Own-Consumption Rate

The own-consumption rate (OCR) is calculated as shown in Eq. 8:

$$OCR = \frac{\text{own consumed PV energy}}{\text{Total PV generation}} \cdot 100 \quad (8)$$

The OCR consists of the ratio of own-consumed PV energy and the total generated PV energy spanning the entire observation period.

2.3 Energy System Modeling and Linear Optimization

2.3.1 Open Energy Modeling Framework

For the modeling of the sector-integrated energy system, the open energy modeling framework (*oemof*) was used [30]. With the help of different *oemof* libraries, activities such as the generation of load time series can be undertaken and sector-integrated energy systems can be modeled and optimized. We used the *oemof.solph* library [31]. *Oemof.solph* functions as a wrapper for the *Pyomo* Python library [32], which can be used to solve linear optimization problems. Different solvers can be employed. In this study, the *CBC* solver (coin-or-branch and cut) was used [33]. The structure of *oemof.solph* is based on the components: *Sink*, *Source*, *Bus*, *LinearTransformer*, and *GenericStorage*. All components were connected by so-called *Flows*. A system of linear equations, with constraints if necessary, was then set up for a modeled energy system and minimized to its total cost by the solver. Further information on the individual *oemof.solph* components and optimization can be found in [34] and [35].

2.3.2 The Investigated Energy System

The description of the basic model of the energy system with *oemof* components and all technical and economic parameters can be traced in [18], with Fig. 1, Fig. 3, and the following describing the aspects that have been changed or added in this study.

The electrical connection of the property is limited to 240 kVA. The PV and battery storage system no longer has a fixed nominal power but only a maximum of 150 kW_p PV power and 150 kWh storage capacity.

In addition to the existing energy system from [18], an further cold sector was integrated. The cooling demand (Table 2) is covered by chillers and a 1000 m³ cold water storage (CWS) unit. The chiller is modeled as a *LinearTransformer* with a pre-calculated time series of the EER in accordance with [36]. For the modeling of the CWS, the *oemof.solph* component *GenericStorage* is used. The storage has an assumed conversion factor of 90% during charging and discharging. The nominal storage capacity

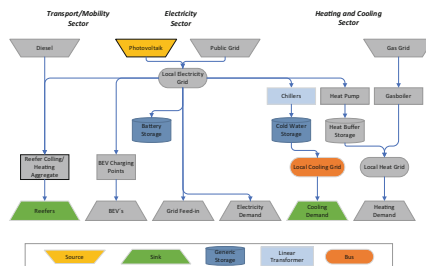


Fig. 3. Investigated sector-integrated distributed energy systems in *oemof.solph* components. The gray components were adapted from [18].

is given by Eq. (9):

$$CWS_{nom} = V_{Water} \cdot \rho_{Water} \cdot C_{Water} \cdot (T_{high} - T_{Low}) \tag{9}$$

where V_{Water} is the water volume, ρ_{Water} the water density, C_{Water} the heat capacity of water, T_{high} the maximum water temperature (12 °C), and T_{Low} the minimum temperature (6 °C).

The relative losses of the storage are given by the loss rate LR in Eq. 10:

$$LR_{CWS} = \frac{U_{Iso} \cdot A_{Surface}}{V_{Water} \cdot \rho_{Water} \cdot C_{Water} + A_{Surface} \cdot S_{Iso} \cdot \rho_{Iso} \cdot C_{Iso}} \tag{10}$$

where U_{Iso} is the U-Value of the isolation, $A_{Surface}$ the surface of the buffer storage, S_{Iso} the insulation thickness, ρ_{Iso} the insulation density, and C_{Iso} the insulation heat capacity.

For computing the time reduction, a simplified model of the reefers was introduced for this study, contrasting with [18]. Hereby, the power demands for pre-cooling or pre-heating of all reefers present at the facility were aggregated. Thus, instead of optimizing each connection individually, the aggregated demand of the sum of all pre-cooling and -heating processes was determined. The principal structure of the modeling of a reefer with *oemof.solph* components is shown in Fig. 4 and described in more detail in [18].

Each reefer has a maximum electrical connected load of 13.2 kW in cooling and 8.8 kW in heating mode. The presence times on the property can be taken from Fig. 5. Here, the probabilities of which day of the week the reefers are at the site are also presented.

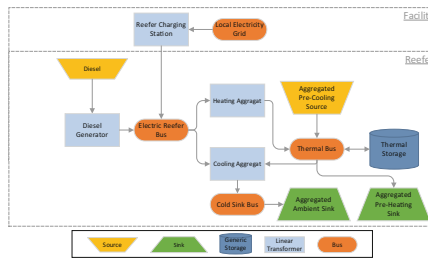


Fig. 4. Reefer modeling of the oemof.solph components, according to [18].

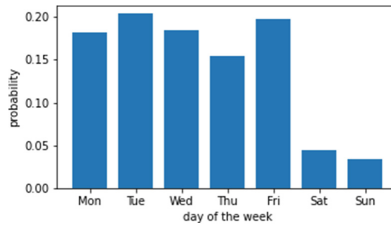


Fig. 5. Reefer attendance times on the property for preconditioning processes [18].

2.4 Design Optimization

PyGMO was developed for parallel optimization and can be used to solve different kinds of optimization problems, such as single or multiple target problems or those with or without constraints. With the help of the asynchronous, generalized island model, evolutionary algorithms and other algorithms can be easily mixed and adapted to an optimization problem [37]. In comparison to traditional genetic algorithms (GAs), the generalized island model operates with the idea of different subcultures that live on different islands. The possibility of recombination between any two individuals becomes restricted. Recombination is now limited to individuals of the sub-culture of one island. On each island, a different GA with different optimization parameters can be utilized. Solutions can be exchanged in a so-called migration process. At certain points in time, a migration operation is used to select individuals from one island to send them to another and introduce them to a foreign population [38]. For the design optimization, *PyGMO* [37] in combination with *oemof.solph* was used, as shown in Fig. 6.

The process can be described as follows: The first step is to generate the energy system model using *oemof.solph* components (Sect. 2.2). In the second step, the multi-objective design optimization problem is implemented with *PyGMO*, on top of the energy system one.

It was first determined how the archipelago should look and how many generations per evolutionary step should be passed through. The parameters used in this study are shown in Table 7.

In this case study, three islands were used and each of them ran a different algorithm. The algorithms NSGA2, MACO, and NSPSO utilized are further described in [39]. For each individual, i.e., a dimensioning of the PV and battery storage system, an operation

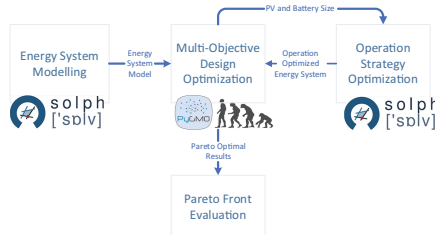


Fig. 6. Flow-chart of the multi-objective design optimization approach.

Table 7. Parameter overview of the multi-criteria design optimization with *PyGMO* [37].

Islands	3
Algorithms [39]	NSGA2, MACO, NSPSO
Population size	24
Number of generations	3
Evolutionary steps	100

Table 8. Pareto-optimal results of the design optimization for PV and battery storage size.

Scenario	PV Size [kW]		Battery Storage Capacity [kWh]	
	SIES	CES	SIES	CES
Pareto-optimal solutions	7626	9948	7626	9948
Mean	105.34	100.68	50.26	67.61
First quartile (Q1)	77.61	77.89	8.54	23.45
Median	114.07	109.70	37.97	64.24
Third quartile (Q3)	136.64	132.44	81.41	107.30

optimization was performed with *oemof.solph*. The evaluation of the KPIs takes place in a third step. The KPIs are then fed back into the evolutionary algorithms mentioned previously. The result of this evolution is multiple Pareto-optimal (i.e., no particular KPI can be improved without worsening another one) component dimensioning's.

3 Results

3.1 Multi-objective Design Optimization Results

The design optimization yields 7626 Pareto-optimal results from a total of 21,600 optimization runs in the SIES and 9948 for the CES scenario (Table 8). Unless otherwise stated, all units should be understood as units per observation period.

For the SIES scenario, the median PV size is 114 kW and for the interquartile range (first to third quartile), it ranges from 78 to 137 kW of installed capacity (see also Table 8).

The interquartile range of the battery storage capacity ranges from 8.58 to 81 kWh, with a median of 32.54 kWh in the SIES scenario.

Comparing the size design of the CES with the SIES using boxplots, differences quickly become apparent (Table 8 and Fig. 7). The box marks the interquartile range between the first and third quartile of all values, whereas the orange line marks the median values. The lowest point of the whisker indicates the minimum value, whereas the highest point of the whisker represents the maximum value.

Figure 7 shows the comparison results of the design optimization scenarios for a PV system and battery storage. The interquartile range for the PV system is very similar and the median is on the same level. With respect to storage size, the interquartile range of the CES scenario is higher and the median is about 27 kWh apart.

3.2 Pareto-Front Evaluation of the Sector-Integrated Energy System

How the individual KPIs affect the sizes of the battery capacity and storage size is shown in Fig. 8 and Fig. 9.

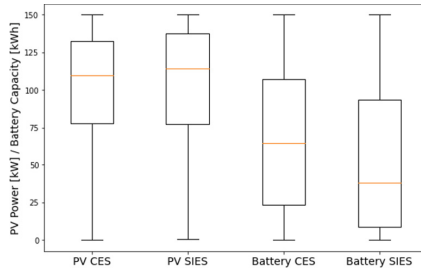


Fig. 7. Evaluation of the Pareto-optimal design results of the PV system size and battery storage capacity.

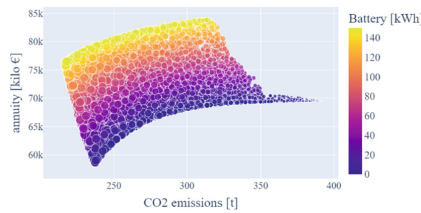


Fig. 8. Analysis of the Pareto-front of the KPIs of annuity and CO₂ emissions from the sector-integrated energy system scenario. The color gradient indicates the size of the storage capacity (from small: dark blue, to large: light yellow), whereas the size of the circles shows the size of the installed PV power.

Fehler! Verweisquelle konnte nicht gefunden werden. Displays the relationship between annuity and CO₂ emissions. It can be seen that a large PV system with a substantial battery capacity produces the lowest emissions, but results in the highest annuity. With a very small battery capacity but a large PV system, the annuity is the lowest and CO₂ emissions increase only slightly. Looking at the color gradient on the left edge, it is clear that the battery size and annuity in particular are positively correlated. However, the PV size has the greatest impact on emissions, which becomes clear when looking at the lower horizontal line (only very small storage capacities) from left to right (increasing circles or PV sizes). With a virtually unchanged storage size, the emissions increase with decreasing PV size.

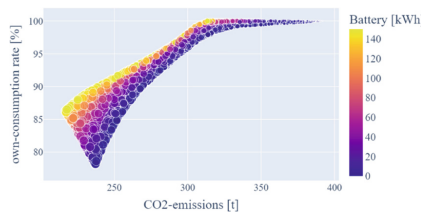


Fig. 9. Analysis of the Pareto-front of the KPIs of own-consumption rate and CO₂ emissions from the sector-integrated energy system scenario.

Table 9. Statistical comparison of KPIs between conventional and sector-integrated energy systems.

	Annuity in k€	CO ₂ emissions in t	Own-consumption rate in %
Mean	70.48	266.64	90.24
25%	66.20	237.53	85.52
50%	70.11	254.33	89.66
Median			
75%	75.03	289.81	95.63

Figure 9 shows the relationship between CO₂ emissions and the OCR. Large battery capacities (yellow) and PV plant size (large circles) result in decreasing OCR. Emissions of up to 85% OCR. On the left side it is shown that with maximum storage size and PV, no greater OCR than about 86% is possible, but a decrease in storage capacity (dark blue) leads to an increase in CO₂ emissions.

A statistical summary of the SIES scenario KPIs of all Pareto-optimal results is presented in Table 9.

3.3 Optimized Sector-Integrated Energy System Operation and Reefer Integration

Due to the simplified reefer model, the runtime of each *oemof.solph* optimization can be significantly reduced. Thus, an optimization run with single reefer models requires 287 s and can, with the simplified model, be reduced to only 101 s. This time only corresponds to the pure optimization time from *oemof.solph* and does not include building the model or loading the datasets. Taking all factors into account, the computing time can be reduced by a factor greater than ten. For the design optimization of the PV and battery storage system, it is not important to have recorded each single reefer, but to have aggregated the power. This generates additional costs (capacity charges) at the grid connection point, which is considered in the operation optimization in *oemof.solph* and varies depending on the PV and storage system's size.

To investigate the effect of PV and battery storage on the distributed energy system and reefer integration, three different Pareto optimal results were selected and analyzed. For this purpose, a result with large PV and no storage (C1), small PV and large storage (C2), and a medium size (C3) each were analyzed (see Table 10). As a reference case, optimization is performed without PV and battery storage.

For cases C1-C3, individual linear operation optimizations with *oemof.solph* were performed. The load behaviour at the grid connection point and at the sub-distribution to the reefers was evaluated, to see the effect of the PV and battery.

The load duration curve in Fig. 10 shows that a high PV power without storage has the highest peak loads (blue line, reference and orange line, C1). However, a large PV (C1) can reduce the permanent load. The use of a battery storage (C2 and C3) reduces the peak load and the continuous load compared to the reference case.

Table 10. Selected results for which extra operating strategy optimization is performed.

	PV in kW	Battery in kWh	Annuity in k€	CO ₂ -emissions in t	OCR In %
C1	145.0	0.0	59.4	239.2	79.3
C2	56.1	141.0	83.1	314.8	99.0
C3	80.6	80.2	76.3	285.8	95.6

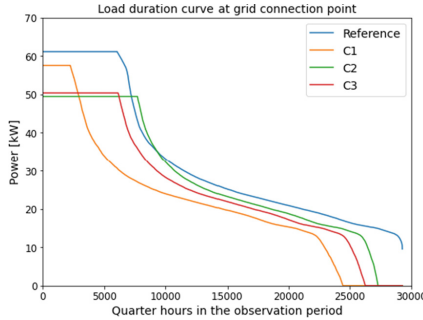


Fig. 10. Load duration curve of cases C1 and C2 and the reference case.

Table 11. Maximum peak loads at reefer connection point.

	Ref.	C1	C2	C3
Peak Load at Reefer Connection Point [kW]	48.44	63.29	113.73	113.73

At the connection point of the reefers, looking at the maximum load peaks shows the effect of PV and battery storage Table 11.

The maximum load peaks (Table 11) show which high loads are possible within the local grid using a battery storage and or PV (C1, C2 and C3) and without loading the house connection point (Fig. 10). In particular, the use of a battery storage system enables high peak loads (C2 and C3).

4 Discussion

In the previous chapter, the results of the design optimization of a PV and storage system were presented and evaluated based on three KPIs.

For the analysis of the Pareto-optimal results of the variables, a comparison between a SIES and CES was performed. The difference in the optimal results of the PV system’s size is only marginal. Due to an increased electrical energy demand through the provision of heat by a heat pump and transport demand through BEVs and reefers, the plant size increases on average by only 5 kW, compared to the CES scenario (Table 8). The slight

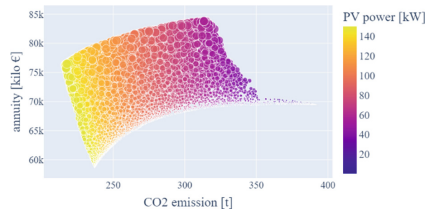


Fig. 11. Impact of PV on the KPIs of annuity and CO₂ emissions. The circles here represent the battery storage capacity size within the Pareto-front.

increase can be explained by the increased electrical energy demand. However, the fact that this is so low can be understood if we examine the KPIs.

The comparison of the annuity and the degree of own-consumption (Fig. 11) shows that the increase in the degree of own-consumption is disproportionately costly for a large system.

Only in the design of the storage capacity do major differences between the scenarios become apparent. The deviation of the mean values is around 14 kWh and the median is 27 kWh when comparing the scenarios. The storage capacity is larger in the case of the CES. The increased electrical demand in the SIES scenario increases self-consumption, even without battery storage. Thus, the storage system can be designed to be somewhat smaller, which reduces the annuity without worsening the other KPIs.

What is only considered in the linear optimization of the *oemof.solph* model is the minimization of load peaks by penalizing additional purchasing power at the connection point. With the conversion of cars to BEVs and reefers from diesel to electric, this aspect naturally presents many challenges, especially when several reefers and BEVs are present at the same time and so high load peaks can occur.

By using a battery storage, it is possible to absorb high power peaks of e.g. reefers. This can have advantages in operation when preconditioning processes have to be fast and many processes have to be carried out simultaneously. As the analysis of the load behavior at the grid connection point and reefer connection point shows, the use of PV and battery storage offers the possibility to reduce peak loads and thus grid charges. In addition, the battery storage in particular provides flexibility so that high load peaks within the local grid are also possible.

An analysis of how a different number of preconditioning reefers at a logistics site affects peak loads and how these can be reduced via optimized schedules was performed by the authors in [18].

5 Conclusions and Outlook

In this study, an approach was presented by means of which it is possible to carry out the design of distributed generation and storage with multi-criteria objectives. In the case study of the decentralized energy system of a logistics property, in which the conventional diesel-powered transportation system and heat supply are electrified, a design optimization for a PV and storage system was conducted. Three KPIs were introduced for this purpose: the annuity, CO₂ emissions, and degree of own-consumption rate. The

energy system was modeled based on a previous work [18] that employed *oemof.solph*. A runtime-optimized reefer model was developed for the electrical preconditioning processes of reefers into a sector-integrated system. For the multi-criteria design, the Python library *PyGMO* was introduced. In total, 21,600 optimizations were performed. Only the Pareto-optimal solutions were used for analyzing the results. By comparing a conventional (CES) and sector-integrated energy system (SIES), the influence of sector-coupling on design optimization could be demonstrated.

Based on the Pareto-optimal results, a configuration of PV and battery capacities can be selected depending on the needs of the energy system's stakeholders, e.g., whether the emissions of a company or the annuity are the focus. These results can then be used to perform an operating strategy optimization using linear optimization and the energy system model in *oemof.solph*. The combination of *oemof.solph* and *PyGMO* allows the design of much more complex power systems and the optimization of their operating strategies. Ultimately, it is a question of computing capacity.

In further analyses, other KPIs can also be selected, such as the minimization of load peaks, primary energy demand, and maximizing the degree of self-sufficiency, which becomes intriguing again in times of uncertain energy price developments. In addition, this method can also be used for larger energy systems and a variety of technologies. Examples are given by Schmelling et al. [16].

For the optimization of the energy systems operation or operating strategies of flexible loads and producers, the *oemof.solph* model should be extended to include a prediction-based operation optimization. For real world application, a prediction-based model with uncertainty quantification would be necessary. For design optimization, evaluation of results and estimation of energy requirements, the presented approach is highly suitable.

Acknowledgements. The authors would like to acknowledge financial support from the “Federal Ministry for Economic Affairs and Climate Action” of the Federal Republic of Germany for the project: “ELogZ: Energieversorgungskonzepte für klimaneutrale Logistikzentren” (03EN1015F). For more details, visit www.elogz.de. The presented study was conducted as part of this project. A special thanks is also due to Paneuropa Transport GmbH (<https://paneuropa.com/>) for the provision of data and knowhow.

Authors' Contributions. **Jan-Simon Telle:** Conceptualization, Methodology, Software, Data Curation, Visualization, Writing - Original Draft; **Sunke Schlüters:** Software, Methodology, Data Curation, Writing - Review & Editing, Project administration; **Thomas Poppinga:** Conceptualization, Writing - Review & Editing, Validation, Project administration; **Benedikt Hanke:** Conceptualization, Writing - Review & Editing, Supervision, Funding acquisition; **Karsten von Maydell:** Investigation, Funding acquisition, Review & Editing; **Carsten Agert:** Supervision, Funding acquisition, Review & Editing.

References

1. G. Fridgen, R. Keller, M.-F. Körner and M. Schöpf, “A holistic view on sector coupling,” *Energy Policy (Volume 147)*, December 2020.

2. M. Robinius, A. Otto, P. Heuser, L. Welder, K. Syranidis, D. S. Ryberg, T. Grube, P. Markewitz, R. Peters and D. Stolten, "Linking the Power and Transport Sectors—Part 1: The Principle of Sector Coupling," *energies*, 2017.
3. M. Robinius, A. Otto, K. Syranidis, D. S. Ryberg, P. Heuser, L. Welder, T. Grube, P. Markewitz, V. Tietz and D. Stolten, "Linking the Power and Transport Sectors—Part 2: Modelling a Sector Coupling Scenario for Germany," *energies*, 2017.
4. T. Haas and H. Sander, "Decarbonizing Transport in the European Union: Emission Performance Standards and the Perspectives for a European Green Deal," *sustainability*, 2020.
5. Federal Ministry of Justice Germany, *Brennstoffemissionshandelsgesetz - BEHG*, 2019.
6. European Parliament, *Directive 2003/87/EC of the European Parliament and of the Council of 13 October 2003 establishing a scheme for greenhouse gas emission allowance trading within the Community and amending Council Directive 96/61/EC (Text with EEA relevance)*, European Union, 2003.
7. Applus+ IDIADA, TM Leuven Transport & Mobility, TU Graz, "Bodies and trailers – development of CO2 emissions determination procedure; Procedure no: CLIMA/C.4/SER/OC/2018/0005," European Commission, 2018.
8. B. Sharper and F. Rodriguez, "MARKET ANALYSIS OF HEAVY-DUTY COMMERCIAL TRAILERS IN EUROPE," The International Council on Clean Transportation (icct), Washington, DC, 2018.
9. Statistisches Bundesamt, "Lange Preisreihen für leichtes Heizöl, Motorenbenzin und Dieselmotoren - Juli 2022," 12 08 2022. [Online]. Available: <https://www.destatis.de/DE/Themen/Wirtschaft/Preise/Erzeugerpreisindex-gewerbliche-Produkte/Publikationen/Downloads-Erzeugerpreise/erzeugerpreise-preisreihe-heizoeel-pdf-5612402.html>. [Accessed 17 08 2022].
10. CE Delft (Co-financed by the European Union), "Electrical trailer cooling during rest periods - Analysis of emissions and costs," CE Delft, Delft, 2015.
11. A. Rai, "Energy demand and environmental impacts of food transport refrigeration and energy reduction methods during temperaturecontrolled distribution - PhD Thesis," Brunel University London - College of Engineering, Design and Physical Sciences, London, 2019.
12. J. Baartmans, *Refrigerated Trailer: Electricity or Diesel (Bachelor Thesis)*, Erasmus University Rotterdam; Department: Urban Port and Transport Economics, 2015.
13. B. Steden, J.-S. Telle, N. Wollek, S. Schlütters and J. Marx Gómez, "Distributed Sector Coupled Low Carbon Energy Supply for Logistics Properties – Concept for the Integration of Heating, Electricity and Transport," in *Environmental Informatics – A bogeyman or saviour to achieve the UN Sustainable Development Goals? - Adjunct Proceedings of the 35th edition of the EnviroInfo*, Berlin, 2021.
14. A. Rai and S. A. T. Tassou, "Energy demand and environmental impacts of alternative food transport refrigeration systems," in *The 15th International Symposium on District Heating and Cooling Energy demand and environmental impacts of alternative food*, Berkshire, UK Berkshire UK, 2017.
15. A. Rai and S. A. Tassou, "Environmental impacts of vapour compression and cryogenic transport refrigeration technologies for temperature controlled food distribution," *Energy Conversion and Management*, no. 150, pp. 914-923, 2017.
16. Schmeling, Lucas; Schönfeldt, Patrik; Klement, Peter; Vorspel, Lena; Hanke, Benedikt, Hanke; von Maydell, Karsten; Agert, Carsten, "(Preprint) A generalised optimal design methodology for distributed energy systems," *TechRxiv*, p. <https://doi.org/10.36227/techrxiv.19426745.v1>, 30 03 2022.

17. P. Schönfeldt, "Techno-socio-economic energy system optimization.," 15 03 2022. [Online]. Available: http://www.fze.uni-saarland.de/AKE_Archiv/DPG2022-AKE_Erlangen.online/Vortraege/DPG2022_AKE2.2_.Schoenfeldt_EnergySystem-ParetoOptimized.pdf. [Accessed 25 08 2022].
18. J.-S. Telle, S. Schlüters, P. Schönfeld, H. Bendeikt, K. von Maydell and C. Agert, "[Accepted Paper] The Optimized Integration of Temperature-Controlled Transports into Distributed Sector-Integrated Energy Systems," *Energy Conversion and Management*, 08 2022.
19. "ELogZ - Energieversorgungskonzepte für klimaneutrale Logistikzentren," Carl von Ossietzky Universität Oldenburg, [Online]. Available: <https://elozg.de/>. [Accessed 17 09 2021].
20. W. F. Holmgren, C. W. Hansen and M. A. Mikofski, "pvlib python: a python package for modeling solar energy systems," *Journal of Open Source Software*, 2018.
21. Deutscher Wetterdienst, "Open DWD," [Online]. Available: <https://opendata.dwd.de/>. [Accessed 23 06 2021].
22. L. Reinholdt, J. Kristófersson, B. Zühlsdorf, B. Elmegaard, J. Jensen, T. Ommen and P. H. Jørgensen, "Heat pump COP, part 1: Generalized method for screening of system integration potentials," in *Proceedings of the 13th IIR-Gustav Lorentzen Conference on Natural Refrigerants*, <https://doi.org/10.18462/iir.gl.2018.1380>, 2018.
23. Verein Deutscher Ingenieure e.V., *VDI 2061 - Part 1, Economic efficiency of building installations - Fundamentals and economic calculation*, Düsseldorf: Beuth Verlag GmbH, 2012.
24. "EEG register data and reference values for payment," [Online]. Available: https://www.bundesnetzagentur.de/SharedDocs/Downloads/DE/Sachgebiete/Energie/Unternehmen_Institutionen/ErneuerbareEnergien/ZahlenDatenInformationen/PV_Datenmeldungen/DegressionsVergSaetze_08-10_21.html?nn=654268. [Accessed 08 08 2022].
25. German Federal Office of Justice, "Gesetz für den Ausbau erneuerbarer Energien (Erneuerbare-Energien-Gesetz - EEG 2021)," 16 07 2021. [Online]. Available: https://www.gesetze-im-internet.de/eeg_2014/EEG_2021.pdf. [Accessed 02 02 2022].
26. Bundesnetzagentur, "EEG register data and reference values for payment," [Online]. Available: <https://www.bundesnetzagentur.de/EN/Areas/Energy/Companies/RenewableEnergy/RegisterDataTariffs/start.html;jsessionid=E97371F37AF2029EAF3FE133A99434>. [Accessed 07 02 2022].
27. BSW - Bundesverband Solarwirtschaft e.V., "Direktvermarktung von Solarstrom - Markt- und Anbieterübersicht," Bundesverband Solarwirtschaft e.V.
28. Umweltbundesamt, "CO2 emissions per kilowatt hour of electricity in further decline in 2019," Umweltbundesamt, 08 April 2020. [Online]. Available: <https://www.umweltbundesamt.de/presse/pressemittelungen/bilanz-2019-co2-emissionen-pro-kilowattstunde-strom>.
29. juris GmbH, "Verordnung über die Emissionsberichterstattung nach dem Brennstoffemissionshandelsgesetz für die Jahre 2021 und 2022 (Emissionsberichterstattungsverordnung 2022 - EBeV 2022) - Anlage 1 (zu den §§ 5, 6, 10 und 11) - Ermittlung der Brennstoffemissionen," Bundesamt für Justiz - Kompetenzzentrum Rechtsinformationssystem des Bundes, [Online]. Available: http://www.gesetze-im-internet.de/ebev_2022/anlage_1.html.
30. S. Hilpert, C. Kaldemeyer, U. Krien, S. Günther, C. Wingenbach and G. Plessmann, "The Open Energy Modelling Framework (oemof) - A new approach to facilitate open science in energy system modelling," *Energy Strategy Reviews*, no. 22, pp. 16-25, 2018.
31. U. Krien, P. Schönfeld, J. Launer, S. Hipert, C. Kaldemeyer and G. Pleßmann, "oemof.solph— A model generator for linear and mixed-integer linear optimisation of energy systems," *Software Impacts*, 11 2020.
32. M. L. Bynum, G. A. Hackebeil, W. E. Hart, C. D. Laird, B. L. Nicholson, J. D. Sirola, J.-P. Watson and D. L. Woodruff, *Pyomo--optimization modeling in python*, Springer, 2017.

33. J. Forrest, T. Ralphs, H. G. Santos, S. Vigerske, L. Hafer, B. Kristjansson, jpfasano, Edwin-Straver, M. Lubin, rlougee, jpgoncal1, Jan-Willem, h-i-gassmann, S. Brito, Cristina, M. Saltzman, tosttost and F. MATSUSHIMA, *coin-or/Cbc: Release releases/2.10.7*, DOI: <https://doi.org/10.5281/ZENODO.5904374>, 2022.
34. oemof developer group, “oemof.solph,” oemof developer group, [Online]. Available: <https://github.com/oemof/oemof-solph>. [Accessed 20 06 2022].
35. oemof-developer-group, “oemof documentation,” oemof-developer-group, 2014–2021. [Online]. Available: <https://oemof-solph.readthedocs.io/en/latest/usage.html#solph-components>. [Accessed 20 06 2022].
36. oemof developer group, “oemof.thermal,” oemof developer group, [Online]. Available: https://oemof-thermal.readthedocs.io/en/latest/absorption_chillers.html.
37. F. Biscani and D. Izzo, “A parallel global multiobjective framework for optimization: pagmo,” *Journal of Open Source Software*, p. 2238, 2020.
38. D. Izzo, M. Rucinski and F. Biscani, “The Generalized Island Model,” in *Parallel Architectures and Bioinspired Algorithms*, 2012, pp. 151–169.
39. D. Izzo and F. Biscani, “PyGMO - User Documentation - Algorithms,” [Online]. Available: <https://esa.github.io/pygmo/documentation/algorithms.html>. [Accessed 09 08 2022].

Open Access This chapter is licensed under the terms of the Creative Commons Attribution-NonCommercial 4.0 International License (<http://creativecommons.org/licenses/by-nc/4.0/>), which permits any noncommercial use, sharing, adaptation, distribution and reproduction in any medium or format, as long as you give appropriate credit to the original author(s) and the source, provide a link to the Creative Commons license and indicate if changes were made.

The images or other third party material in this chapter are included in the chapter’s Creative Commons license, unless indicated otherwise in a credit line to the material. If material is not included in the chapter’s Creative Commons license and your intended use is not permitted by statutory regulation or exceeds the permitted use, you will need to obtain permission directly from the copyright holder.

